Development of a non-toxic and non-denaturing formulation process for encapsulation of SDF-1α into PLGA/PEG-PLGA nanoparticles to achieve sustained release

Muhammad Haji Mansor, Mathie Najberg, Aurélien Contini, Carmen Alvarez-Lorenzo, Emmanuel Garcion, Christine Jérôme, Frank Boury

Accepted Manuscript

Muhammad Haji Mansor, Mathie Najberg, Aurélien Contini, Carmen Alvarez-Lorenzo, Emmanuel Garcion, Christine Jérôme, Frank Boury

Development of a Non-toxic and Non-denaturing Formulation Process for Encapsulation of SDF-1α into PLGA/PEG-PLGA Nanoparticles to Achieve Sustained Release

Muhammad Haji Mansor[a,b], Mathie Najberg[a,c], Aurélien Contini[a], Carmen Alvarez-Lorenzo[c], Emmanuel Garcion[a,*], Christine Jérôme[b,*], Frank Boury[a,#]

[a]CRCINA, INSERM, Université de Nantes, Université d'Angers, Angers, France
[b]Center for Education and Research on Macromolecules (CERM), Université de Liège, Liège, Belgium
[c]Departamento de Farmacologia, Farmacia y Tecnología Farmacéutica, R & D Pharma Group, Facultad de Farmacia, Universidade de Santiago de Compostela, Santiago de Compostela, Spain

* Equivalent contribution

Corresponding author.
E-mail address: frank.boury@univ-angers.fr
Tel: +33 (0)2 44 68 85 28 / +33 (0)6 19 39 49 59 (mobile)
Fax: +33 (0)2 02 44 68 85 46
Postal address:
Cancer and Immunology Research Centre Nantes-Angers (CRCINA)
INSERM U1232, Team GLIAD
Université d'Angers
IBS - CHU Angers
4 rue Larrey
49933 ANGERS CEDEX 9, France

Keywords:

1. Introduction

Stromal cell-derived factor-1α (SDF-1α)[1] is a chemokine composed of 68 amino acids [1] that binds to its cognate receptor, C-X-C chemokine receptor type 4 (CXCR4) [2]. One of its important physiological functions is to retain high concentrations of CXCR4-expressing stem and progenitor cells within the bone marrow by creating a positive concentration gradient from the blood to this organ [3]. In the events of tissue damage, the SDF-1α expression at the injury site is elevated [4–6] in a simultaneous fashion to the increased SDF-1α degradation in the bone marrow [7,8] to allow mobilisation of the stem and progenitor cells and their subsequent chemoattraction to the site of damage. In addition to its roles in tissue repair and regeneration, SDF-1α-mediated chemotaxis is also implicated in tumour metastases. CXCR4-expressing cancerous cells that are present in the blood or lymphatic circulation after getting dislodged from the primary tumour site can be chemoattracted to SDF-1α-secreting sites such as the bone marrow [9], liver [10] and lymph nodes [11] for future metastatic growth. This pathological role of SDF-1α has inspired the design of implants capable of creating a SDF-1α concentration gradient for trapping CXCR4-expressing cancerous cells relevant to multiple types of malignant cancers such as glioblastoma (GBM) [12], gastric carcinoma [13] and small-cell lung cancer [14].

---

[1] **List of abbreviations:**
AFM: atomic force microscopy, BSA: bovine serum albumin, CXCR4: C-X-C chemokine receptor type 4, DL: drug loading, DMEM: Dulbecco's Modified Eagle's Medium, DMI: isosorbide dimethyl ether/dimethyl isosorbide, DMSO: dimethyl sulfoxide, EE: encapsulation efficiency, ELISA: enzyme-linked immunosorbent assay, FBS: foetal bovine serum, GBM: glioblastoma, HCl: hydrochloric acid, HPBCD: hydroxypropyl-β-cyclodextrin, ICH: International Conference on Harmonization, LNC: lipid nanocapsules, Mn: number-average molecular weight, Mw: weight-average molecular weight, NaCl: sodium chloride, NIH3T3: mouse fibroblast cell line NIH3T3, NMR: nuclear magnetic resonance, P188: poloxamer 188, PBS: phosphate-buffered saline, PDI: polydispersity index, PE: precipitation efficiency, PEG: polyethylene glycol, pI: isoelectric point, PLGA: poly-lactic-co- glycolic acid PLGA-COOH: poly-lactic-co- glycolic acid with uncapped carboxylic acid terminals, PLGA-COOR: poly-lactic-co- glycolic acid with capped carboxylic acid terminals, PS: polystyrene, PVA: polyvinyl alcohol, SD: standard deviation, SDF-1α: stromal cell-derived factor-1α, SEC: size exclusion chromatography, SEM: scanning electron microscopy, T_c: collapse temperature, TEM: transmission electron microscopy, Tris: tris(hydroxymethyl)-aminomethane, U87-MG: human malignant glioblastoma cell line U87-MG

Due to its solubility and rapid diffusion in physiological media, a sustained delivery of SDF-1α is a prerequisite for establishing its concentration gradient. Encapsulation of SDF-1α into polymeric nanoparticles is a credible strategy for achieving a gradual SDF-1α release at the site of application. In this regard, poly-(lactic-co-glycolic acid) (PLGA) is a polymer of choice for nanoparticle formulations, owing to its biocompatibility, biodegradability and most importantly, its status as a Food and Drug Administration-approved pharmaceutical excipient [15]. However, due to its hydrophobicity, the formation of stable PLGA nanoparticles often necessitates the use of amphiphilic surfactants such as polyvinyl alcohol (PVA) [16,17] and poloxamer 188 (P188) [18] in the formulation process. Although these surfactants are innocuous when used in isolation, residual PVA and P188 bound to the PLGA nanoparticle surfaces have been reported to induce toxicities especially at nanoparticle concentrations exceeding 1 mg/mL [19], which are relevant to many local applications of PLGA-based nanoparticles. The development of a PLGA-based nanoparticle formulation process that avoids or reduces the need for surfactants is therefore in demand.

To encapsulate hydrophilic drugs in hydrophobic PLGA matrices, the double emulsion (water/oil/water) process is often preferred [20,21]. While this process is excellent for encapsulating small hydrophilic molecules, problems can arise with drugs of complex structures such as proteins. The first step of this process that involves emulsification of a protein solution in the polymer-containing organic phase can lead to adsorption of protein molecules to the water/organic solvent interface and their subsequent unfolding. The structural instability of dissolved proteins is actually exaggerated by their conformational flexibility that makes it possible for their hydrophobic pockets to be externalised to make contact with the organic phase upon emulsification [22]. Thus, a possible solution to promote protein stability during encapsulation is by minimising their conformational mobility through the use of proteins in solid form. In this regard, techniques such as freeze-drying and spray-freeze-drying have been employed to produce fine protein particles for subsequent encapsulation [23,24]. However, these techniques themselves can induce substantial protein structural changes. On the other hand, proteins in solution can be precipitated by adding a water-

miscible organic solvent [25]. This technique produces homogenous nano-sized protein particles without affecting protein structures and bioactivities, and therefore serves as a suitable protein treatment prior to encapsulation.

Currently, the encapsulation of proteins or peptides into PLGA nanoparticles typically involves the use of toxic halogenated solvents such as chloroform and dichloromethane as the polymer solvent [26–28]. Other common harmful PLGA solvents include acetonitrile [29], N-methylpyrrolidone [30], N,N-dimethylformamide and tetrahydrofuran [31]. These solvents belong to Class 2 according to the International Conference on Harmonization (ICH), which are harmful solvents that can pose serious threats to patient safety [32]. Less toxic solvents such as acetone [33], ethyl acetate [34] and dimethyl sulfoxide [30] are being increasingly used as alternatives. Nevertheless, they are still regarded as potential hazards to human health by the ICH. Differently, the safety of non-volatile water-miscible organic solvents such as glycofurol and isosorbide dimethyl ether (DMI) have been demonstrated *in vivo.* They have been recommended as solvents suitable for intravascular injections [35,36] due to their negligible toxicity. Thus, the use of these solvents for protein encapsulation into PLGA-based nanoparticles is well-motivated.

In the present study, an amphiphilic polyethylene glycol (PEG)-PLGA co-polymer was synthesised and used together with hydrophobic PLGA polymers to produce stable nanoparticles via a phase separation method without the use of conventional surfactants. In addition, the non-toxic DMI was utilised as a solvent for the PLGA polymers and the PEG-PLGA co-polymer. To the best of our knowledge, this is the first example of the use of this benign solvent to produce PLGA/PEG-PLGA nanoparticles. PLGA with capped or uncapped carboxylic acid terminals were combined with the PEG-PLGA co-polymer at different proportions to produce nanoparticles of different size distributions and surface charges. The nanoparticles were then freeze-dried in the presence of three excipients to explore the possibility of obtaining nanocarriers with a prolonged shelf-life. Following the optimisation of the PLGA/PEG-PLGA nanoparticle synthesis, lysozyme (14.3 kDa, isoelectric

point: 11.35) was initially used as a model protein to optimise the encapsulation of SDF-1α (8.0 kDa, isoelectric point: 10.5). To preserve the protein bioactivity throughout the formulation process, lysozyme and SDF-1α precipitates were prepared by mixing respective protein solutions with glycofurol prior to encapsulation. Then, *in vitro* release of lysozyme and SDF-1α from the PLGA/PEG-PLGA nanoparticles was studied. The bioactivity of the released SDF-1α was subsequently assessed in terms of its capacity to induce migration of CXCR4-expressing human GBM cells (U87-MG). Finally, the cytocompatibility of the newly-developed nanoparticles was assessed *in vitro*.

2. Materials and methods

2.1. Materials

PLGA with capped carboxylic acid terminals and PEG-PLGA co-polymer were synthesised as described in Section 2.2.. PLGA 75:25 with uncapped terminals (Resomer® RG752H, Mw = 9850 Da, polydispersity index (PDI) = 2.4), lysozyme of chicken egg white, *Micrococcus lysodeikticus*, glycofurol (tetraglycol or tetrahydrofurfuryl alcohol polyethyleneglycol ether), isosorbide dimethyl ether (dimethyl isosorbide), dimethyl sulfoxide (DMSO), sodium chloride, poloxamer 188 (Lutrol® F68), glycine, sucrose, trehalose, 37% hydrochloric acid, 10 M sodium hydroxide, tris(hydroxymethyl)aminomethane (Tris) base (Trizma®) and agarose with low gelling temperature were obtained from Sigma-Aldrich (Saint Quentin Fallavier, France). DL-lactide (Purasorb® DL) and glycolide (Purasorb® G) were obtained from Purac Biomaterials, Frankfurt, Germany. Bovine serum albumin fraction V was obtained from Roche Diagnostics (Mannheim, Germany), human SDF-1α from Miltenyi Biotech (Paris, France), hydroxypropyl-β-cyclodextrin (Kleptose® HPBCD) from Roquette (Lestrem, France), Dulbecco's phosphate-buffered saline (Biowhittaker®) from Lonza (Verviers, Belgium), and Dulbecco's Modified Eagle's Medium (Gibco® DMEM) from Thermo Fisher Scientific (Villebon sur Yvette, France). Ultrapure water dispensed from a Milli-Q® Advantage A10 system (Millipore, Paris, France) was used in all experiments.

2.2. Synthesis and characterization of PLGA with capped carboxylic acid terminals (PLGA-COOR) and PEG-PLGA co-polymer

2.2.1. Synthesis

The synthesis of PLGA-COOR was adapted from the ring-opening polymerization method described by Yoo and Park [37]. Briefly, a mixture of DL-lactide (Purasorb® DL) and glycolide (Purasorb® G) in the molar ratio of 3:1 was heated with the initiator benzyl alcohol to 140 °C under nitrogen atmosphere for complete melting. The use of this initiator would result in a benzyl group being the

R-group in the PLGA-COOR product. Then, 0.04% (w/w) stannous octoate was added, and the reaction mixture was further heated to 180 °C. The temperature was maintained for 3 hours for polymerization to take place under static vacuum. The polymer was then recovered by dissolution in dichloromethane before precipitation in heptane. The precipitate was subsequently filtered and dried at 25 °C for 24 hours under vacuum. For the synthesis of PEG-PLGA co-polymer, the same procedure was adopted except that monomethoxy-PEG of number average molecular weight (Mn) of 5 kDa (Sigma-Aldrich) was used as an initiator instead of benzyl alcohol, and the precipitation of PEG-PLGA was carried out in diethyl ether chilled to -20 °C.

2.2.2. Characterization

^{1}H nuclear magnetic resonance (^{1}H-NMR) spectra were recorded using a Bruker Avance® 400 apparatus (Bruker, Brussels, Belgium) to characterise the polymer/co-polymer composition and to estimate Mn. Deuterated DMSO and chloroform were used as solvents for PLGA-COOR and PEG-PLGA co-polymer respectively. Spectra were recorded at 400 MHz in the Fourier Transform mode at 25 °C with chemical shifts expressed in ppm with respect to the tetramethylsilane standard. The polymer/co-polymer was also characterized by size exclusion chromatography (SEC) using a Viscotek® TDA-305 equipment (Malvern, Worcestershire, UK). Polymer/co-polymer was dissolved in tetrahydrofuran at 5 mg/mL for elution at a flow rate of 1 mL/min at 45 °C. The weight-average molecular weight (Mw) and Mn were expressed with respect to polystyrene standards. The PDI of the polymer/co-polymer was subsequently obtained by calculating the ratio of Mw to Mn.

2.3. Preparation of lysozyme and SDF-1α precipitates

Proteins were precipitated using a technique adapted from Giteau et al. [25]. Briefly, lyophilized protein as provided by the supplier was dissolved in sodium chloride (NaCl) solution containing 20% (w/v) P188 as a protein protective agent. 25 μL of the protein solution was then added to 975 μL glycofurol in a 10 mL Nalgene® Oak Ridge High-Speed centrifuge tube (Thermo Fisher Scientific) prior to incubation in ice for 30 minutes. The optimal concentrations of protein and NaCl were

investigated initially using lysozyme as a model protein. To evaluate the precipitation efficiency (PE), the formed suspension of protein precipitates was centrifuged at 12,800 x g for 30 minutes. The supernatant was carefully discarded and the pelleted protein precipitates were dissolved in 1 mL 0.05 M Tris-HCl buffer solution containing 0.1% (w/v) bovine serum albumin (BSA) and diluted for further quantification (see Section 2.7.). PE was calculated using Equation 1.

$$PE\ (\%) = \frac{Mass\ of\ protein\ recovered\ after\ precipitation}{Initial\ mass\ of\ protein\ used\ as\ a\ starting\ material}\ x\ 100 \qquad \text{(Equation 1)}$$

2.4. Preparation of lysozyme- and SDF-1α-loaded nanoparticles

Nanoparticles were formed using a phase separation method adapted from Tran et al. [17]. Briefly, PLGA-COOR, PLGA-COOH and PEG-PLGA co-polymer were dissolved separately in DMI at 12% (w/v). The three polymer solutions were mixed in different proportions to give a total volume of 300 µl. For protein encapsulation, 100 µl protein precipitate suspension in glycofurol consisting of either 25 µg lysozyme or 10 µg SDF-1α was added to the polymer solutions prior to magnetic stirring at 1300 rpm for 30 seconds. The theoretical drug loadings (DL), as calculated using Equation 2, were 0.07 % and 0.03 % for lysozyme and SDF-1α respectively. For the synthesis of unloaded nanoparticles, the 100 µl protein precipitates was replaced with an equal volume of glycofurol alone. Then, 100µl aqueous phase in the form of 0.05 M glycine-NaOH buffer solution was added under magnetic stirring to initiate phase separation. After 1 minute, another 500µl aqueous phase was added every 30 seconds for four times to enhance the phase separation process. The pH of the aqueous phase was varied to investigate the effect of protein solubility on encapsulation efficiencies. The formed nanoparticle suspension was diluted with water to 30 mL to allow diffusion of residual solvents out of the nanoparticles. After 1 hour, the nanoparticle suspension was centrifuged for 30 minutes at 10,000 x g. The supernatant was discarded and the nanoparticle pellet was re-suspended in water. The centrifugation was repeated once to complete the purification process and the resultant nanoparticle suspension was concentrated to a final volume of 1 mL.

$$DL\ (\%) = \frac{Initial\ mass\ of\ protein\ used\ as\ a\ starting\ material}{Total\ mass\ of\ PLGA\ and\ PEG-PLGA}\ x\ 100 \qquad \text{(Equation 2)}$$

2.5. Freeze-drying of nanoparticles

After purification, 1 mL of nanoparticle suspension was transferred into a 20 mL glass vial. To ensure the stability of the nanoparticles throughout the freeze-drying process, 1 mL of cryoprotectant solution was added to the nanoparticle suspension to give a total volume of 2 mL and a final nanoparticle concentration of approximately 15 mg/mL. The cryoprotectants tested were HPBCD, trehalose and sucrose, at a final concentration of 5% (w/v). The vial was then immersed in liquid nitrogen (-196 °C) for 1 minute to freeze the nanoparticle-cryoprotectant mixture, and subsequently placed on the shelf of the freeze-dryer pre-cooled to -35 °C for 2 hours. The samples were subsequently lyophilized, alongside cryoprotectant-free nanoparticle samples as a control, in a Lyovax® GT freeze-dryer (Steris, Bordeaux, France) at -20 °C and 0.3 mbar for 16 hours. The nanoparticle size was measured (as described in 2.6.1.) before and after freeze-drying. The nanoparticles were assumed to be stable throughout the freeze-drying process if the ratio of final to initial size (S_f/S_i) and polydispersity index (PDI_f/PDI_i) is close to 1.

2.6. Nanoparticle characterization

2.6.1. Size distribution and zeta-potential

The nanoparticle size distribution was determined by a dynamic light scattering (DLS) technique whereas zeta-potentials were derived from electrophoretic mobility values using the Smoluchowski's approximation. Nanoparticle samples were prepared by dilution in water or 0.01 M NaCl solution for size and zeta-potential measurements respectively, to obtain concentrations suitable for analyses in a Nanosizer® ZS (Malvern) such that the attenuator value was in the range of 5 - 7. Each sample was measured in triplicate, with each measurement representing an average value of at least 10 runs. All measurements were made at 25°C under automatic mode. Besides average particle size, the DLS

protocol of Nanosizer® ZS produced a PDI value ranging between 0 – 1 that estimates the width of the size distribution.

2.6.2. Scanning electron microscopy (SEM), transmission electron microscopy (TEM) and atomic force microscopy (AFM)

The nanoparticle morphology was visualised under SEM (JSM 6310F, JEOL, Paris, France), TEM (JEM 1400, JEOL, Paris, France) and AFM (AutoProbe CP-Research, Veeco Digital Instruments, Santa Barbara, California, USA). A 2 µL drop of purified nanoparticle suspension at a concentration of 200 µg/mL was added onto the centre of a glass slide (for SEM and AFM) or carbon-coated nickel grid (for TEM), and left to dry overnight at room temperature. For SEM, the sample was coated with a gold layer of 5 nm thickness prior to observation while no coating was applied to TEM or AFM samples. For AFM, tapping mode (resonance frequency = 300 kHz) was used instead of contact mode to minimise sample damage upon observation.

For the observation of protein nanoprecipitates, the undiluted protein nanoprecipitate suspension was used to prepare samples for SEM, via the same procedure as the preparation of nanoparticle samples.

2.6.3. Protein encapsulation efficiency

Lyophilized protein-loaded nanoparticles, and unloaded nanoparticles as a control, were dissolved in 1 mL DMSO for 1 hour before the addition of 3 mL 0.01 M HCl. The solution was left to stand for another hour for protein extraction from the nanoparticle fragments. The samples were then diluted for use in protein quantification assays (see Section 2.7.). Encapsulation efficiency (EE) was calculated using Equation 3.

$$EE\ (\%) = \frac{Mass\ of\ protein\ recovered\ from\ dissolved\ nanoparticles}{Initial\ mass\ of\ protein\ used\ as\ a\ starting\ material}\ x\ 100 \qquad \text{(Equation 3)}$$

2.7. Protein quantification

2.7.1. Quantification of lysozyme

Lysozyme was quantified using *Micrococcus lysodeikticus* cell suspension as a substrate as described by Morille et al. [38]. Briefly, 100 µL lysozyme solution or sample was added to 2.9 mL suspension of *M. lysodeikticus* (0.015% (w/v)) in 0.05 M Tris-HCl buffer solution (pH 7.4). After 4 hours of incubation at 37°C, the absorbance was measured at 450 nm. For the construction of a standard curve, the concentration of lysozyme solutions used was between 100 - 1000 ng/mL. 0.05 M Tris-HCl buffer solution (pH 7.4) was used to prepare several dilutions of the samples to obtain absorbance readings that were within the standard curve range.

2.7.2. Quantification of SDF-1α

SDF-1α was quantified using an enzyme-linked immunosorbent assay (ELISA) according to the supplier's instructions (R&D Systems, Lille, France). Briefly, SDF-1α capture antibody solution was added to a Nunc Maxisorp® 96-well microplate (Thermo Fisher Scientific) and incubated overnight to coat the wells. The microplate was then washed with 0.05% (w/v) Tween® 20 in phosphate-buffered saline (PBS) solution (pH 7.4), followed by a 1-hour incubation with PBS solution (pH 7.4) containing 1% (w/v) BSA to block the microplate. After washing, the kit standard and samples diluted in PBS (pH 7.4) containing 1% (w/v) BSA were added to the microplate for a 2-hour incubation. Then, the microplate was washed before addition of a detection antibody solution for another 2-hour incubation. The washing step was subsequently repeated prior to incubation with a streptavidin-horseradish peroxidase solution for 20 minutes. After the final wash, a substrate solution was added for another 20-minute incubation. Finally, 2 N sulphuric acid was added to terminate the enzymatic reaction followed by immediate measurement of absorbance at 450 nm. All incubations were done at room temperature.

2.8. Assessment of SDF-1α bioactivity

The bioactivity of the precipitated and released SDF-1α was assessed using the agarose drop migration assay as adapted from Milner et al. [39]. Briefly, U87-MG cells (American Tissue Culture Collection, Rockville, Maryland, USA), previously transfected to express CXCR4 receptor by Séhédic et al. [40], were seeded into a 24-well flat-bottomed culture plate (Nunc, Strasbourg, France) at a density of 1×10^5 cells per well and cultured in medium supplemented with 10% foetal bovine serum (FBS) and 1% penicillin/streptomycin. The wells were previously treated with 500 μL of a 10 μg/mL poly-D-lysine hydrobromide (Sigma-Aldrich) solution for 15 minutes at 37 °C and washed three times with PBS prior to cell seeding. After 72 hours of incubation at 37 °C under a 5% CO_2 humidified atmosphere , the culture medium was removed and the cells were lysed by adding water (500 μL per well) to cover the well surfaces with a thin cell-derived matrix. After 20 minutes, the wells were washed three times with PBS and allowed to air-dry. Then, 2 μL of 1% (w/v) low gelling point agarose solution containing U87-MG cells at a density of 50×10^6 cells/mL was dropped onto the centre of each well and allowed to gel at 4 °C for 15 minutes. At this point, 400 μL of SDF-1α-free medium or medium supplemented with 40 ng/mL native/precipitated/released SDF-1α was added to the cell-laden agarose drops prior to incubation. After 72 hours, optical microscopic images of the plan view of each well were taken. Cell migration was estimated by measuring the distance between the furthest-migrating cells and the edge of the cell-laden agarose drop. Measurements were made on four sides (north, east, south and west) of the drop using ImageJ software and subsequently averaged to obtain a representative value of a drop. Three drops were prepared for each medium condition in each experiment.

2.9. *In vitro* protein release

Protein-loaded nanoparticles, and unloaded nanoparticles as a control, were suspended in 2 mL buffer solution containing 0.1% (w/v) BSA as a protein stabilizer and kept in a 2 mL centrifuge tube. The tube was incubated at 37°C in a shaking water bath (125 rpm). At pre-defined time intervals, the tube was centrifuged at 8500 *x g* for 30 minutes. 0.3 mL of the supernatant was collected and

replaced with fresh buffer. The supernatant was stored at -20 °C until protein quantification (as described in Section 2.7 for lysozyme and SDF-1α) and biological activity assessment (as described in Section 2.8 for SDF-1α).

2.10. *In vitro* cytotoxicity of nanoparticles

In vitro cytotoxicity of unloaded PLGA/PEG-PLGA nanoparticles was evaluated using a resazurin-based assay adapted from Swed et al. [41]. NIH3T3 mouse fibroblast cell line was cultured at 37 °C and 5% CO_2 in medium supplemented with 10% FBS and 1% penicillin/streptomycin, and replaced every 3 days. The cells were seeded in a 96-well flat-bottomed culture plate (Nunc) at a density of 5.5×10^3 cells/well in 100 µL medium and incubated at 37 °C and 5% CO_2 for 24 h. At this point, 50 µL of the old medium was replaced with an equal volume of nanoparticle-containing fresh medium, to obtain final nanoparticle concentrations of 0.01, 0.1, 1 and 10 mg/mL. As a negative control, cells incubated with the medium alone were prepared. After 48 h of incubation (72 h post-seeding) in the presence or absence of nanoparticles, the entire medium was replaced with 100 µL fresh medium containing 44 µM resazurin. The resazurin-containing medium was also added in three wells of the assay plates (without cells), which served as blank. The plate was incubated for another 3 h 30 m. Cell viability was estimated from the fluorescence intensity of the reduced product of resazurin, called resorufin, which was measured using a ClarioStar microplate fluorometer (BMG Labtech GmbH, Ortenberg, Germany) at 545 nm excitation and 600 nm emission. All readings were normalised to those obtained with the nanoparticle-untreated cells.

In addition to the PLGA/PEG-PLGA nanoparticles, two other types of nanoparticles, namely lipid nanocapsules (LNC) and polystyrene (PS) nanoparticles, were tested in this assay to obtain information on the relative safety of the newly-developed nanoparticles. LNC (average size = 122 nm, PDI = 0.088) were prepared using a phase inversion method as discussed by Heurtault et al. [42]. PS nanoparticles (average size = 285 nm, PDI = 0.175) were purchased from Sigma-Aldrich.

2.11. Statistical analysis

Data are presented as the mean value ± standard deviation (SD) of at least three experiments (n ≥ 3). One-way ANOVA with post-Dunnet's multiple comparison test with a threshold P-value of 0.05 was used to investigate any significant difference between multiple groups of data. In the figures, * indicates P ≤ 0.05, ** indicates P ≤ 0.01, *** indicates P ≤ 0.001 and **** indicates P ≤ 0.0001.

3. Results and discussion

3.1. Characterization of PLGA-COOR and PEG-PLGA co-polymer

^{1}H-NMR spectrum of PLGA-COOR in Figure 1 revealed the presence of lactide units at 5.19 ppm and 1.46 ppm, glycolide units at 4.91 ppm, and benzyl capping groups at 7.37 ppm. Using the signal at 7.37 ppm as a reference for integration, Mn was calculated to be 5.5 kDa, with a lactide/glycolide molar percentage of 75/25. For the PEG-PLGA co-polymer, the signal at 3.64 ppm, which is characteristic of ethylene glycol units, indicated the successful co-polymerization of monomethoxy-PEG 5 kDa to the lactide and glycolide units. Using this signal as a reference, the Mn of the co-polymer was 30.7 kDa (PEG 5 kDa - PLGA 25.7 kDa) whereas the lactide/glycolide molar percentage was calculated to be 75/25. On the other hand, SEC analyses showed that the Mw/Mn values were 11.2/5.7 kDa (PDI = 2.0) and 44.1/21.0 kDa (PDI = 2.1) for PLGA-COOR and PEG-PLGA co-polymer respectively. The disparity between the PEG-PLGA Mn values calculated using these two techniques could be attributed to the amphiphilic nature of the co-polymer [38,43,44] that may have modified the hydrodynamic volume to prolong the retention time, which subsequently produced an underestimated Mn value using SEC.

[Insert Figure 1]

3.2. Lysozyme and SDF-1α precipitation

Due to the greater stability of proteins in their solid state, proteins dissolved in a salt solution containing P188 were precipitated through their addition to an organic solvent as a preparation for encapsulation. Glycofurol was the organic solvent of choice for two main reasons. Firstly, its water-miscibility enables an efficient separation of water from protein molecules to induce precipitation. Secondly, it has been used to precipitate many proteins without causing their denaturation [25,38,45,46]. P188 was added due to its ability to refold any unfolded protein [47] and also to reduce protein adsorption to the hydrophobic PLGA following encapsulation, which in turn may

allow for greater cumulative release [38,48]. To minimise any potential toxicity, the amount of P188 used to precipitate the amount of protein sufficient for one nanoparticle formulation was kept at 500 µg. Proteins were initially dissolved in NaCl solution to neutralise the charged protein molecules and promote attractive hydrophobic interactions. The concentration of NaCl that would decrease the aqueous solubility of SDF-1α without causing its denaturation was investigated using lysozyme as a model protein. Following precipitation, the amount of bioactive lysozyme was quantified using the *Micrococcus lysodeikticus* assay. As shown in Figure 2, 0.15 M NaCl resulted in a successful precipitation with a complete preservation of lysozyme bioactivity. Lower PE was obtained in the absence of NaCl, possibly due to the repulsion between charged protein molecules that hindered the formation of precipitates. On the other hand, PE decreased when the NaCl concentration was increased above 0.15 M. Although high concentrations of salt can reduce the aqueous solubility of a protein and facilitate precipitation, the excess charge neutralisation may simultaneously promote protein denaturation by allowing any unfolded protein molecules to spontaneously form aggregates and therefore preventing their re-folding [49]. On this basis, 0.15 M NaCl was used to precipitate SDF-1α. The effect of protein concentrations on PE was also investigated. PE values were greater with higher lysozyme concentrations, due to greater tendencies for protein molecules to collide and interact with one another. Although 10 mg/mL or higher lysozyme concentrations were identified to result in a maximum PE, it was not possible to dissolve SDF-1α in 0.15 M NaCl at these concentrations. Therefore, SDF-1α was precipitated at 2.67 mg/mL, which was the highest concentration that could be achieved without the appearance of visible protein solids. Using ELISA, the PE was calculated to be 91 ± 5%. More importantly, the bioactivity of the re-constituted SDF-1α precipitates was not significantly different from the native SDF-1α when tested using the agarose drop migration assay (Figure 6B,C).

Following the optimisation of precipitation conditions, the morphology of the precipitates was observed under SEM. The precipitates of both proteins were mostly spherical in shape (Figure 3). Furthermore, their size distributions (as estimated using the ImageJ software) were 57 ± 10 nm and

57 ± 25 nm for lysozyme and SDF-1α respectively. The sub-100 nm sizes of the protein precipitates make them ideal for subsequent encapsulation into the PLGA/PEG-PLGA nanoparticles.

[Insert Figure 2]

[Insert Figure 3]

3.3. Preparation and characterization of lysozyme- and SDF-1α-loaded nanoparticles

3.3.1. Optimisation of PLGA/PEG-PLGA nanoparticle synthesis

Due to the amphiphilic behaviour of PEG-PLGA, it was predicted that uniform and stable nanoparticles can be obtained by mixing this co-polymer with the hydrophobic PLGA. Using this combination instead of the co-polymer alone can provide additional means for controlling the nanoparticle physicochemical properties that are critical for protein encapsulation and release, such as the size and zeta-potential, by varying the chemical constituents of the PLGA component such as the number of uncapped carboxylic acid groups.

The physicochemical characteristics of unloaded nanoparticles made from different combinations of PEG-PLGA co-polymer and PLGA polymers are shown in Table 1. No homogeneous nanoparticle suspension could be obtained in the absence of PEG-PLGA (Formulations 1 & 5) whereas the size and PDI values decreased as the PEG-PLGA proportion was increased when used in combination with either PLGA-COOH (Formulations 2 - 4) or PLGA-COOR (Formulations 6 - 8). These observations confirmed the critical nanoparticle-stabilizing roles of the co-polymer to compensate for the lack of use of surfactants such as PVA and P188. Furthermore, zeta-potential values generally became less negative with increasing PEG-PLGA proportion, which can be explained by the increasing density of PEG layer on the nanoparticle surface that shields the negatively-charged PLGA carboxylic acid groups [50]. Based on these observations and literature data [51], the synthesised nanoparticles can be thought of to possess a structure consisting of a hydrophilic PEG layer surrounding a hydrophobic PLGA core.

Upon substituting PLGA-COOH with an equal proportion of PLGA-COOR, the nanoparticle size increased and zeta-potential values became less negative (Formulations 2 vs. 6, 3 vs. 7 and 4 vs. 8), which suggested that PLGA terminal capping has an effect on nanoparticle properties. To confirm this, PLGA-COOH and PLGA-COOR were combined with a fixed proportion of PEG-PLGA that is sufficient to produce uniform nanoparticles (Formulation 9 and 10). Taking together the results obtained when only either PLGA-COOH or PLGA-COOR was combined with PEG-PLGA (Formulations 4 and 8), it was confirmed that the nanoparticle size increased as the PLGA-COOH was gradually replaced with PLGA-COOR. Simultaneously, the zeta-potential values also became less negative. The largest zeta-potential change was seen in alkaline conditions (pH 10) due to deprotonation of all uncapped carboxylic acid groups. The greater abundance of uncapped carboxylic acid terminals found in nanoparticles made of higher PLGA-COOH proportions may lead to higher inter-particle electrostatic repulsions, which prevent particle collusion and consequently reduce the average size.

[Insert Table 1]

To ensure good colloidal stability, zeta potential values of greater than +30 mV or lower than -30 mV are generally regarded as ideal, as this ensures strong electrostatic repulsive forces between the nanoparticles [52]. In this work, the presence of the external PEG layer inevitably decreased the zeta potential magnitude of the PLGA/PEG-PLGA nanoparticles. Despite the loss in electrostatic stabilization, the nanoparticle suspension benefited from the steric stabilization conferred by the PEG chains. To verify this, Formulation 8 was suspended in 0.05 M Tris-HCl buffer (pH 7.4) containing 0.15 M NaCl at 1 mg/mL concentration and the suspension was kept at 37 °C. There were minimal changes in the average size of the nanoparticles after 20 days (Supplementary Figure 1A). Interestingly, the zeta-potential values became increasingly negative with time (Supplementary Figure 1B). It was likely that PEG-mediated steric repulsions provided the main stabilization force for freshly-produced nanoparticles. As the PLGA ester bonds gradually hydrolyzed to reveal more

negatively-charged carboxylic acid terminals, the increasing magnitude of electrostatic repulsions prevented the formation of any aggregates.

3.3.2. Freeze-drying of PLGA/PEG-PLGA nanoparticles

Polyesters such as PLGA are prone to degradation by means of hydrolysis of the ester bonds, which may lead to leakage of the drug load encapsulated within polyester-based nanocarriers. Therefore, dehydration of PLGA-based nanoparticles, commonly by freeze-drying, is imperative to ensure their long-term stability. To protect the nanoparticles from freezing and drying stresses, cryoprotectants should be added to the nanoparticle suspension before freezing. Disaccharides such as sucrose and trehalose, and oligosaccharides such as HPBCD have been shown to be excellent protectants [53]. Nevertheless, it is also important that the drying temperature is maintained below the collapse temperature (T_c) of the protectant to prevent the collapse of the freeze-dried products [54], which may lead to prolonged nanoparticle reconstitution times [53,55] and higher residual humidity [56].

In this study, 5% (w/v) sucrose, trehalose and HPBCD with T_c of -32, -30 and -15 °C respectively [57,58] were used as protectants. The shelf temperature throughout the drying phase was fixed at -20 °C as this was the lowest temperature for water vaporization at 0.3 mbar, which was the lowest pressure achievable by the freeze-dryer used in this study. As predicted, the freeze-dried product containing either sucrose or trehalose appeared collapsed and required sonication for reconstitution while the non-collapsed HPBCD-stabilised product could be reconstituted completely by gentle agitation alone. The formulation collapse resulted in a decrease in the degree of porosity of the freeze-dried product, which subsequently reduced its surface area to volume ratio and hydration rate [56]. Nevertheless, all three protectants produced better results compared to that obtained from the lyophilization of nanoparticle suspension alone, confirming the protective roles of these excipients during freeze-drying.

Following reconstitution, the nanoparticle size and PDI were measured again to evaluate the protective effect of sucrose, trehalose and HPBCD. The highest protective effect, as demonstrated by

the maximum preservation of nanoparticle size and PDI, was obtained with HPBCD (Table 2). It is likely that the volume shrinkage resulting from the collapse of the sucrose and trehalose matrices has reduced the distance of separation between the nanoparticles, allowing the PEG layers of neighbouring particles to interact and form stable crystalline bridges as reported in the literature [51,59]. Differently, in the presence of HPBCD, the PLGA/PEG-PLGA nanoparticles were easily freeze-dried, which may be convenient for long-term storage and transportation. In future work, the protective effects of sucrose and trehalose can be re-evaluated by setting the drying temperature to be lower than their respective T_c to minimise dependency on the relatively costly HPBCD.

[Insert Table 2]

3.3.3. Lysozyme and SDF-1α encapsulation

3.3.3.1. Effect of pH of the aqueous phase on encapsulation efficiencies

Protein molecules have smaller net electrical charge and thus lower aqueous solubility when the pH is buffered near the protein's isoelectric point (pI). This may decrease the leakage of protein into the aqueous phase during the formulation process to subsequently maximise encapsulation efficiency. The results shown in Table 3 supported this hypothesis as both lysozyme and SDF-1α were encapsulated most successfully when the pH of the aqueous phase was buffered closest to their respective pI (lysozyme – 11.35; SDF-1α – 10.5). In addition to a decrease in aqueous solubility, it is likely that the smaller net charge also attenuated the electrostatic repulsions between protein molecules to allow the protein load to be compacted, which can facilitate its entrapment within the nanoparticles [60,61]. For these reasons, the pH of the aqueous phase was always set to the protein's pI in subsequent encapsulations.

[Insert Table 3]

3.3.3.2. Effect of PLGA carboxylic acid terminal capping on encapsulation efficiencies

Since both proteins and PLGA possess ionisable groups, electrostatic interactions can have a major influence on lysozyme and SDF-1α encapsulation. Due to the complexity associated with protein charge modifications, the proportions of PLGA-COOH and PLGA-COOR were altered accordingly to vary the number of ionisable groups in the nanoparticles instead. The encapsulation of both proteins decreased slightly when PLGA-COOH was substituted with an equal amount of PLGA-COOR (Formulation 4 vs. 8 in Table 4). These results suggested that protein-polymer electrostatic interactions can influence the protein encapsulation efficiencies. Although protein leakage during the encapsulation process can be minimised by adjusting the pH of the aqueous phase to be similar to the protein's pI, proteins located close to the nanoparticle surface can be lost during subsequent purification stages when the nanoparticles were suspended in non-buffered water. This is especially true since the presence of the outer hydrophilic PEG layer can facilitate the access of water to the PLGA core to cause dissolution of any loosely-trapped proteins [62]. However, the strong electrostatic interactions between the negatively-charged carboxylic acid terminals, which are more abundant in PLGA-COOH than in PLGA-COOR, and the positively-charged basic proteins such as lysozyme and SDF-1α can reduce protein loss. Interestingly, additional experiments with lysozyme (Formulation 9 and 10) and SDF-1α (Formulation 10) produced similar results as Formulation 4. Considering the very low protein loading involved, it seems that the inclusion of a small proportion of PLGA-COOH is sufficient to ensure that the nanoparticles have an adequate number of carboxylic acid groups to interact with the protein molecules for maximum encapsulation efficiency.

[Insert Table 4]

3.3.3.3. Physicochemical characteristics of protein-loaded nanoparticles

Protein encapsulation did not affect the size or zeta-potential of the nanoparticles regardless of the type of formulation or encapsulated protein (Table 5), possibly due to the low amount of protein being encapsulated. In terms of morphology, both the unloaded and SDF-1α-loaded nanoparticles appeared similar under the vacuum condition of SEM or TEM (Figure 4). In addition, the image taken

using AFM under a non-vacuum condition confirmed the consistent appearance of the SDF-1α-loaded nanoparticles regardless of the conditions under which the nanoparticles were observed and the differences in the sample treatment prior to observation.

[Insert Table 5]

[Insert Figure 4]

3.4. *In vitro* protein release

Protein release was studied by suspending the nanoparticles in a buffer solution followed by centrifugation at pre-defined time intervals to collect the supernatant for protein quantification. Initially, lysozyme release patterns in different buffer solutions was studied. At the physiologically-relevant pH 7.4 (0.05 M Tris-HCl buffer), the proportion of PLGA-COOH in the nanoparticles was shown to affect the extent of lysozyme release (Figure 5A). The highest release of encapsulated lysozyme was achieved with Formulation 8 (43%) whereas negligible protein release was observed with Formulation 4 even after 15 days. When a mixture of PLGA-COOH and PLGA-COOR was tested (Formulation 10), only 12% encapsulated lysozyme was successfully released. The lack of protein release from PLGA particles containing uncapped carboxylic end groups has been previously reported [38,41,63]. Concurrent measurement of zeta-potentials during the release study offered a possible explanation for this observation. Nanoparticles made from higher PLGA-COOH proportions had more negative zeta-potential values in the early stages of the release study (Figure 5B). At pH 7.4, these nanoparticles are expected to establish electrostatic interactions with the positively-charged lysozyme molecules (pI = 11.35), which hinders their release. These interactions seem to be the governing factor for protein load entrapment, as no further protein release was observed despite the continuous degradation of PLGA matrices into acidic products, as inferred from the increasingly negative zeta-potential values of all the formulations, taking place throughout the release study period.

To confirm the obstructive effect of lysozyme-PLGA electrostatic interactions on lysozyme release, the study was repeated in release medium buffered to pH 4.0 (0.01 M citrate buffer). It can be hypothesised that the excess protons present in the release medium will neutralise the PLGA carboxylic acid groups, which in turn should trigger the release of lysozyme molecules. As expected, release of lysozyme was enhanced regardless of the nanoparticle's PLGA-COOH proportion (Figure 5C). However, incomplete release was still observed with Formulation 4, even after 30 days. It is likely that the high proportion of PLGA-COOH in this formulation led to incomplete neutralisation of the carboxylic acid groups, hindering complete lysozyme release. Besides pH, another factor that may affect lysozyme-PLGA electrostatic interactions is the concentration of cations in the release medium, as these ions can also displace lysozyme molecules from the PLGA carboxylic acid groups. As predicted, in the presence of 0.15 M sodium chloride, release of lysozyme at pH 7.4 was enhanced (Figure 5D), recording levels similar to those obtained at acidic pH. These release medium conditions were selected for subsequent SDF-1α release study due to their physiological relevance.

[Insert Figure 5]

Interestingly, although the biphasic release pattern seen in lysozyme release study was reproduced, the release of SDF-1α was reduced in all formulations (Figure 6A). After 30 days, the nanoparticles were lyophilized and dissolved to quantify the amount of unreleased SDF-1α using ELISA. The sum of released SDF-1α and the unreleased proportion, was equal to 95 – 98% of the total encapsulated SDF-1α for all the studied formulations. SDF-1α may establish stronger electrostatic interactions with PLGA carboxylic acid groups than lysozyme because of the greater percentage of basic amino acid residues in the SDF-1α primary sequence, resulting in lower cumulative SDF-1α releases. Despite the multiple literature-approved measures taken in this study to reduce protein-polymer interactions, including protein precipitation in the presence of poloxamer 188 [38] and use of more hydrophilic polymer materials [63] in the form of PEG-PLGA co-polymer, additional approaches such as protein PEGylation [64,65] should be considered in future work to obtain more complete protein release.

Nevertheless, the bioactivity of SDF-1α in the release sample collected up to 72 hours (after which further SDF-1α release was negligible) was found to be similar to that of its native counterpart when assessed using the agarose drop migration assay (Figure 6B,C), suggesting that the encapsulation process did not induce protein denaturation. In the context of patient safety, the preservation of protein bioactivity throughout formulation processes is imperative as denatured proteins tend to be more immunogenic than their native forms [66,67].

[Insert Figure 6]

The biphasic release patterns observed in lysozyme and SDF-1α release studies were consistent with literature data on PEG-containing PLGA nanoparticles [61,68]. The initial burst release was due to the rapid liberation of proteins located adjacent to the nanoparticle surface, which was a consequence of the efflux of residual solvents during the purification step that drew most proteins away from the core of the nanoparticles. This stage was then followed by a slower release attributable to the diffusion of proteins from deeper parts of the nanoparticles. In relation to future work, the initial rapid SDF-1α release is useful for establishing a concentration gradient within a hydrogel to immediately induce chemotaxis of cancer cells while the subsequent gradual release may be beneficial to maintain the established gradient. It was also observed that the cumulative release curves began to plateau after 72 hours. This relatively short duration of release was expected as the huge surface area to volume ratio of the nanoparticles contributed to a rapid protein release. However, as the SDF-1α-loaded nanoparticles are intended in the future to be incorporated within a hydrogel and not suspended directly in physiological fluids, literature data suggested that the release duration can be prolonged [69], which would allow more time for cancer cells to migrate into the hydrogel/nanoparticle composite implant to be trapped.

3.5. *In vitro* cytotoxicity study

Due to the innocuous nature of the solvent used in the formulation process and the well-reported safety of PLGA, the newly-developed nanoparticles are expected to exhibit negligible cytotoxicity. To

prove this, NIH3T3 mouse embryonic fibroblasts were treated with unloaded PLGA/PEG-PLGA nanoparticles (Formulation 8) for 48 hours. This cell line was chosen as it has been reported to be highly-sensitive to chemical-induced toxicities [70]. Alongside PLGA/PEG-PLGA nanoparticles, lipid nanocapsules (LNC) and polystyrene (PS) nanoparticles, which have been widely utilised in various pharmaceutical research, were tested to investigate the relative cytocompatibility of the newly-developed nanocarriers. The range of nanoparticle concentrations for cell treatment in this study was set to 0.01 - 10 mg/mL to assess the suitability of the PLGA/PEG-PLGA nanoparticles for both systemic and local drug delivery applications. In comparison to the two reference nanoparticles, the PLGA/PEG-PLGA nanoparticles induced minimal cell deaths even at the highest concentration tested (Figure 7). In addition, the LNC was found to be the most toxic between the three types of nanoparticles at high concentrations. Two studies reported similar findings [71,72] and suggested that the high amount of surfactant (up to 2.8% (w/v)) required to stabilise the LNC formulation is responsible for the high toxicity due to the ability of the hydrophilic and hydrophobic components of surfactant molecules to interact with the phosphate groups and fatty acid tails of lipid bilayer respectively to cause disruption of cellular membranes [73]. On the other hand, the PS nanoparticles exhibited intermediate cytotoxicity, possibly due to the lower amount of surfactant used in their formulation (up to 0.5% (w/v) as described by the manufacturer). Although one can speculate that the differences in the cytotoxicity can be attributed to other components of the three types of nanoparticles, as well as to differences in their physicochemical characteristics such as size and surface charge, the surfactant-free formulation process using non-toxic components developed in the present work can undoubtedly produce nanocarriers with excellent biocompatibility that are more suitable for local drug delivery applications compared to several other well-established alternatives.

[Insert Figure 7]

4. Conclusion

This study reports on the development of novel SDF-1α nanocarriers composed of PLGA and a PEG-PLGA co-polymer. Following optimization using lysozyme as a model protein, SDF-1α was successfully precipitated and subsequently loaded into these nanoparticles under mild formulation conditions. SDF-1α was also released in its bioactive conformation in a gradual fashion. Furthermore, by changing the number of uncapped carboxylic acid groups in the PLGA core, the novel formulation process allows the production of nanoparticles with different physicochemical properties that influence encapsulation efficiencies and the extent of protein release. In addition, the use of non-toxic polymers and solvents ensured the excellent biocompatibility of the synthesised nanoparticles. Thus, the novel SDF-1α nanocarriers are promising for future cancer cell trapping applications and will be incorporated into a suitable hydrogel for studying chemotaxis of glioblastoma cells.

DECLARATION OF INTEREST

No conflict of interest exists.

ACKNOWLEDGEMENT

REFERENCES

[1]   M. De La Luz Sierra, F. Yang, M. Narazaki, O. Salvucci, D. Davis, R. Yarchoan, H.H. Zhang, H. Fales, G. Tosato, Differential processing of stromal-derived factor-1alpha and stromal-derived factor-1beta explains functional diversity., Blood. 103 (2004) 2452–2459. doi:10.1182/blood-2003-08-2857.

[2]   M. Janowski, Functional diversity of SDF-1 splicing variants., Cell Adh. Migr. 3 (2009) 243–249.

[3]   T. Sugiyama, H. Kohara, M. Noda, T. Nagasawa, Maintenance of the Hematopoietic Stem Cell Pool by CXCL12-CXCR4 Chemokine Signaling in Bone Marrow Stromal Cell Niches, Immunity. 25 (2006) 977–988. doi:10.1016/j.immuni.2006.10.016.

[4]   T. Kitaori, H. Ito, E.M. Schwarz, R. Tsutsumi, H. Yoshitomi, S. Oishi, M. Nakano, N. Fujii, T. Nagasawa, T. Nakamura, Stromal cell-derived factor 1/CXCR4 signaling is critical for the recruitment of mesenchymal stem cells to the fracture site during skeletal repair in a mouse model, Arthritis Rheum. 60 (2009) 813–823. doi:10.1002/art.24330.

[5]   J. Deng, Z.M. Zou, T.L. Zhou, Y.P. Su, G.P. Ai, J.P. Wang, H. Xu, S.W. Dong, Bone marrow mesenchymal stem cells can be mobilized into peripheral blood by G-CSF in vivo and integrate into traumatically injured cerebral tissue, Neurol. Sci. 32 (2011) 641–651. doi:10.1007/s10072-011-0608-2.

[6]   Y. Kimura, M. Komaki, K. Iwasaki, M. Sata, Y. Izumi, I. Morita, Recruitment of bone marrow-derived cells to periodontal tissue defects, Front. Cell Dev. Biol. 2 (2014) 1–6. doi:10.3389/fcell.2014.00019.

[7]   J.-P. Lévesque, J. Henry, Y. Takamatsu, P.J. Simmons, L.J. Bendall, Disruption of the CXCR4 / CXCL12 chemotactic interaction during ..., J. Clin. Invest. 110 (2003) 187–196. doi:10.1172/JCI200315994.Introduction.

[8]   L. Marquez-Curtis, A. Jalili, K. Deiteren, N. Shirvaikar, A.-M. Lambeir, A. Janowska-Wieczorek, Carboxypeptidase M Expressed by Human Bone Marrow Cells Cleaves the C-Terminal Lysine of Stromal Cell-Derived Factor-1α: Another Player in Hematopoietic Stem/Progenitor Cell Mobilization?, Stem Cells. 26 (2008) 1211–1220. doi:10.1634/stemcells.2007-0725.

[9]   A.M. Roccaro, A. Sacco, W.G. Purschke, M. Moschetta, C. Maasch, D. Zboralski, S. Zöllner, S. Vonhoff, P. Maiso, M.R. Reagan, S. Lonardi, M. Ungari, D. Eulberg, A. Kruschinski, A. Vater, G. Rossi, I.M. Ghobrial, Therapy, 9 (2014) 118–128. doi:10.1016/j.celrep.2014.08.042.SDF-1.

[10]   R. Matsusue, H. Kubo, S. Hisamori, K. Okoshi, H. Takagi, K. Hida, K. Nakano, A. Itami, K. Kawada, S. Nagayama, Y. Sakai, Hepatic stellate cells promote liver metastasis of colon cancer cells by the action of SDF-1/CXCR4 axis., Ann. Surg. Oncol. 16 (2009) 2645–53. doi:10.1245/s10434-009-0599-x.

[11]   J.-P. Zhang, W.-G. Lu, F. Ye, H.-Z. Chen, C.-Y. Zhou, X. Xie, Study on CXCR4/SDF-1alpha axis in lymph node metastasis of cervical squamous cell carcinoma., Int. J. Gynecol. Cancer. 17 (2007) 478–83. doi:10.1111/j.1525-1438.2007.00786.x.

[12]   C.B. Stevenson, M. Ehtesham, K.M. McMillan, J.G. Valadez, M.L. Edgeworth, R.R. Price, T.W. Abel, K.Y. Mapara, R.C. Thompson, CXCR4 expression is elevated in glioblastoma multiforme and correlates with an increase in intensity and extent of peritumoral T2-weighted magnetic resonance imaging signal abnormalities, Neurosurgery. 63 (2008) 560–569. doi:10.1227/01.NEU.0000324896.26088.EF.

[13]   B.-C. Zhao, Z.-J. Wang, W.-Z. Mao, H.-C. Ma, J.-G. Han, B. Zhao, H.-M. Xu, CXCR4/SDF-1 axis is involved in lymph node metastasis of gastric carcinoma., World J. Gastroenterol. 17 (2011) 2389–96. doi:10.3748/wjg.v17.i19.2389.

[14]   M. Burger, A. Glodek, T. Hartmann, A. Schmitt-Gräff, L.E. Silberstein, N. Fujii, T.J. Kipps, J.A. Burger, Functional Expression of CXCR4 (CD184) on Small-Cell Lung Cancer Cells Mediates Migration, Integrin Activation, and Adhesion to Stromal Cells, Oncogene. 22 (2003) 8093–8101. doi:10.1038/sj.onc.1207097.

[15]   F. Danhier, E. Ansorena, J.M. Silva, R. Coco, A. Le Breton, V. Préat, PLGA-based nanoparticles: An overview of biomedical applications, J. Control. Release. 161 (2012) 505–522.

doi:10.1016/j.jconrel.2012.01.043.

[16]   R.M. Mainardes, R.C. Evangelista, PLGA nanoparticles containing praziquantel: Effect of formulation variables on size distribution, Int. J. Pharm. 290 (2005) 137–144. doi:10.1016/j.ijpharm.2004.11.027.

[17]   X. Song, Y. Zhao, W. Wu, Y. Bi, Z. Cai, Q. Chen, Y. Li, S. Hou, PLGA nanoparticles simultaneously loaded with vincristine sulfate and verapamil hydrochloride: Systematic study of particle size and drug entrapment efficiency, Int. J. Pharm. 350 (2008) 320–329. doi:10.1016/j.ijpharm.2007.08.034.

[18]   M.K. Tran, A. Swed, F. Boury, Preparation of polymeric particles in CO2 medium using non-toxic solvents: Formulation and comparisons with a phase separation method, Eur. J. Pharm. Biopharm. 82 (2012) 498–507. doi:10.1016/j.ejpb.2012.08.005.

[19]   N. Grabowski, H. Hillaireau, J. Vergnaud, N. Tsapis, M. Pallardy, S. Kerdine-Römer, E. Fattal, Surface coating mediates the toxicity of polymeric nanoparticles towards human-like macrophages, Int. J. Pharm. 482 (2015) 75–83. doi:10.1016/j.ijpharm.2014.11.042.

[20]   E. Cohen-Sela, M. Chorny, N. Koroukhov, H.D. Danenberg, G. Golomb, A new double emulsion solvent diffusion technique for encapsulating hydrophilic molecules in PLGA nanoparticles, J. Control. Release. 133 (2009) 90–95. doi:10.1016/j.jconrel.2008.09.073.

[21]   J. Liu, Z. Qiu, S. Wang, L. Zhou, S. Zhang, A modified double-emulsion method for the preparation of daunorubicin-loaded polymeric nanoparticle with enhanced *in vitro* anti-tumor activity, Biomed. Mater. 5 (2010) 65002. doi:10.1088/1748-6041/5/6/065002.

[22]   U. Bilati, E. Allémann, E. Doelker, Strategic approaches for overcoming peptide and protein instability within biodegradable nano- and microparticles, Eur. J. Pharm. Biopharm. 59 (2005) 375–388. doi:10.1016/j.ejpb.2004.10.006.

[23]   A. Sánchez, B. Villamayor, Y. Guo, J. McIver, M.J. Alonso, Formulation strategies for the stabilization of tetanus toxoid in poly(lactide-co-glycolide) microspheres, Int. J. Pharm. 185 (1999) 255–266. doi:10.1016/S0378-5173(99)00178-7.

[24]   J. Wang, K.M. Chua, C.H. Wang, Stabilization and encapsulation of human immunoglobulin G into biodegradable microspheres, J. Colloid Interface Sci. 271 (2004) 92–101. doi:10.1016/j.jcis.2003.08.072.

[25]   A. Giteau, M.C. Venier-Julienne, S. Marchal, J.L. Courthaudon, M. Sergent, C. Montero-Menei, J.M. Verdier, J.P. Benoit, Reversible protein precipitation to ensure stability during encapsulation within PLGA microspheres, Eur. J. Pharm. Biopharm. 70 (2008) 127–136. doi:10.1016/j.ejpb.2008.03.006.

[26]   B. Mukherjee, K. Santra, G. Pattnaik, S. Ghosh, Preparation, characterization and in-vitro evaluation of sustained release protein-loaded nanoparticles based on biodegradable polymers, Int. J. Nanomedicine. 3 (2008) 487–496. doi:10.2147/IJN.S3938.

[27]   T. Feczkó, J. Tóth, G. Dósa, J. Gyenis, Optimization of protein encapsulation in PLGA nanoparticles, Chem. Eng. Process. Process Intensif. 50 (2011) 757–765. doi:10.1016/j.cep.2011.06.008.

[28]   X. Jiang, H. Lin, D. Jiang, G. Xu, X. Fang, L. He, M. Xu, B. Tang, Z. Wang, D. Cui, F. Chen, H. Geng, Co-delivery of VEGF and bFGF via a PLGA nanoparticle-modified BAM for effective contracture inhibition of regenerated bladder tissue in rabbits, Sci. Rep. 6 (2016) 20784. doi:10.1038/srep20784.

[29]   M. Morales-Cruz, G.M. Flores-Fernández, M. Morales-Cruz, E.A. Orellano, J.A. Rodriguez-Martinez, M. Ruiz, K. Griebenow, Two-step nanoprecipitation for the production of protein-loaded PLGA nanospheres, Results Pharma Sci. 2 (2012) 79–85. doi:10.1016/j.rinphs.2012.11.001.

[30]   U. Bilati, E. Allémann, E. Doelker, Development of a nanoprecipitation method intended for the entrapment of hydrophilic drugs into nanoparticles, Eur. J. Pharm. Sci. 24 (2005) 67–75. doi:10.1016/j.ejps.2004.09.011.

[31]   L. Tang, J. Azzi, M. Kwon, M. Mounayar, R. Tong, Q. Yin, R. Moore, N. Skartsis, T.M. Fan, R.

Abdi, J. Cheng, Immunosuppressive Activity of Size-Controlled PEG-PLGA Nanoparticles Containing Encapsulated Cyclosporine A, J. Transplant. 2012 (2012) 1–9. doi:10.1155/2012/896141.

[32] EMEA, ICH guideline Q3C (R6) on impurities: guideline for residual solvents, 2003. http://www.ema.europa.eu/docs/en_GB/document_library/Scientific_guideline/2011/03/WC500104258.pdf.

[33] A. Yang, L. Yang, W. Liu, Z. Li, H. Xu, X. Yang, Tumor necrosis factor alpha blocking peptide loaded PEG-PLGA nanoparticles: Preparation and in vitro evaluation, Int. J. Pharm. 331 (2007) 123–132. doi:10.1016/j.ijpharm.2006.09.015.

[34] J. Coleman, A. Lowman, Biodegradable Nanoparticles for Protein Delivery: Analysis of Preparation Conditions on Particle Morphology and Protein Loading, Activity and Sustained Release Properties, J. Biomater. Sci. Polym. Ed. ahead-of-p (2012) 1–23. doi:10.1163/092050611X576648.

[35] O. Dudeck, O. Jordan, K.T. Hoffmann, A.F. Okuducu, K. Tesmer, T. Kreuzer-Nagy, D.A. Rüfenacht, E. Doelker, R. Felix, Organic solvents as vehicles for precipitating liquid embolics: A comparative angiotoxicity study with superselective injections of swine rete mirabile, Am. J. Neuroradiol. 27 (2006) 1900–1906.

[36] A. Boongird, N. Nasongkla, S. Hongeng, N. Sukdawong, W. Sa-Nguanruang, N. Larbcharoensub, Biocompatibility study of glycofurol in rat brains, Exp. Biol. Med. 236 (2011) 77–83. doi:10.1258/ebm.2010.010219.

[37] H.S. Yoo, T.G. Park, Biodegradable polymeric micelles composed of doxorubicin conjugated PLGA – PEG block copolymer, J. Control. Release. 70 (2001) 63–70.

[38] M. Morille, T. Van-Thanh, X. Garric, J. Cayon, J. Coudane, D. Noël, M.C. Venier-Julienne, C.N. Montero-Menei, New PLGA-P188-PLGA matrix enhances TGF-β3 release from pharmacologically active microcarriers and promotes chondrogenesis of mesenchymal stem cells, J. Control. Release. 170 (2013) 99–110. doi:10.1016/j.jconrel.2013.04.017.

[39] R. Milner, G. Edwards, C. Streuli, C. Ffrench-Constant, A role in migration for the alpha V beta 1 integrin expressed on oligodendrocyte precursors., J. Neurosci. 16 (1996) 7240–7252.

[40] D. Séhédic, I. Chourpa, C. Tétaud, A. Griveau, C. Loussouarn, S. Avril, C. Legendre, N. Lepareur, D. Wion, F. Hindré, F. Davodeau, E. Garcion, Locoregional Confinement and Major Clinical Benefit of [188] Re-Loaded CXCR4-Targeted Nanocarriers in an Orthotopic Human to Mouse Model of Glioblastoma, Theranostics. 7 (2017) 4517–4536. doi:10.7150/thno.19403.

[41] A. Swed, T. Cordonnier, A. Dénarnaud, C. Boyer, J. Guicheux, P. Weiss, F. Boury, Sustained release of TGF-β1 from biodegradable microparticles prepared by a new green process in CO2 medium, Int. J. Pharm. 493 (2015) 357–365. doi:10.1016/j.ijpharm.2015.07.043.

[42] B.J.P. Heurtault B., Saulnier P., Pech B., Proust J.E., A novel phase inversion -based process for the preparation of lipid nanocarrier, Pharm. Res. 19 (2002) 875–880.

[43] F. Li, S. Li, M. Vert, Synthesis and rheological properties of polylactide/poly(ethylene glycol) multiblock copolymers, Macromol. Biosci. 5 (2005) 1125–1131. doi:10.1002/mabi.200500143.

[44] A. Harrane, A. Leroy, H. Nouailhas, X. Garric, J. Coudane, B. Nottelet, PLA-based biodegradable and tunable soft elastomers for biomedical applications, Biomed. Mater. 6 (2011) 65006. doi:10.1088/1748-6041/6/6/065006.

[45] A. Swed, T. Cordonnier, A. Dénarnaud, C. Boyer, J. Guicheux, P. Weiss, F. Boury, Sustained release of TGF-??1 from biodegradable microparticles prepared by a new green process in CO2 medium, Int. J. Pharm. 493 (2015) 357–365. doi:10.1016/j.ijpharm.2015.07.043.

[46] S. Kandalam, L. Sindji, G.J.-R. Delcroix, F. Violet, X. Garric, E.M. André, P.C. Schiller, M.-C. Venier-Julienne, A. des Rieux, J. Guicheux, C.N. Montero-Menei, Pharmacologically active microcarriers delivering BDNF within a hydrogel: Novel strategy for human bone marrow-derived stem cells neural/neuronal differentiation guidance and therapeutic secretome enhancement, Acta Biomater. (2016). doi:10.1016/j.actbio.2016.11.030.

[47]   D. Mustafi, C.M. Smith, M.W. Makinen, R.C. Lee, Multi-block poloxamer surfactants suppress aggregation of denatured proteins, Biochim. Biophys. Acta - Gen. Subj. 1780 (2008) 7–15. doi:10.1016/j.bbagen.2007.08.017.

[48]   A. Paillard-Giteau, V.T. Tran, O. Thomas, X. Garric, J. Coudane, S. Marchal, I. Chourpa, J.P. Benoît, C.N. Montero-Menei, M.C. Venier-Julienne, Effect of various additives and polymers on lysozyme release from PLGA microspheres prepared by an s/o/w emulsion technique, Eur. J. Pharm. Biopharm. 75 (2010) 128–136. doi:10.1016/j.ejpb.2010.03.005.

[49]   S. James, J.J. McManus, Thermal and solution stability of lysozyme in the presence of sucrose, glucose, and trehalose, J. Phys. Chem. B. 116 (2012) 10182–10188. doi:10.1021/jp303898g.

[50]   N. Pirooznia, S. Hasannia, A. Lotfi, M. Ghanei, Encapsulation of Alpha-1 antitrypsin in PLGA nanoparticles: In Vitro characterization as an effective aerosol formulation in pulmonary diseases, J. Nanobiotechnol. 10 (2012) 20. doi:10.1186/1477-3155-10-20.

[51]   F. De Jaeghere, E. Allémann, J. Feijen, T. Kissel, E. Doelker, R. Gurny, Freeze-drying and lyopreservation of diblock and triblock poly(lactic acid)-poly(ethylene oxide) (PLA-PEO) copolymer nanoparticles., Pharm. Dev. Technol. 5 (2000) 473–483. doi:10.1081/PDT-100102031.

[52]   S. Honary, F. Zahir, Effect of Zeta Potential on the Properties of Nano - Drug Delivery Systems - A Review (Part 2), Trop. J. Pharm. Al Res. 12 (2013) 265–273. doi:10.4314/tjpr.v12i2.19.

[53]   W. Abdelwahed, G. Degobert, H. Fessi, Investigation of nanocapsules stabilization by amorphous excipients during freeze-drying and storage, Eur. J. Pharm. Biopharm. 63 (2006) 87–94. doi:10.1016/j.ejpb.2006.01.015.

[54]   W. Abdelwahed, G. Degobert, S. Stainmesse, H. Fessi, Freeze-drying of nanoparticles: Formulation, process and storage considerations, Adv. Drug Deliv. Rev. 58 (2006) 1688–1713. doi:10.1016/j.addr.2006.09.017.

[55]   M. Sameti, G. Bohr, M.N. V Ravi Kumar, C. Kneuer, U. Bakowsky, M. Nacken, H. Schmidt, C.M. Lehr, Stabilisation by freeze-drying of cationically modified silica nanoparticles for gene delivery, Int. J. Pharm. 266 (2003) 51–60. doi:10.1016/S0378-5173(03)00380-6.

[56]   S.M. Patel, T. Doen, M.J. Pikal, Determination of End Point of Primary Drying in Freeze-Drying Process Control, AAPS PharmSciTech. 11 (2010) 73–84. doi:10.1208/s12249-009-9362-7.

[57]   W. Abdelwahed, G. Degobert, H. Fessi, A pilot study of freeze drying of poly(epsilon-caprolactone) nanocapsules stabilized by poly(vinyl alcohol): Formulation and process optimization, Int. J. Pharm. 309 (2006) 178–188. doi:10.1016/j.ijpharm.2005.10.003.

[58]   G. Yang, K. Gilstrap, A. Zhang, L.X. Xu, X. He, Collapse temperature of solutions important for lyopreservation of living cells at ambient temperature, Biotechnol. Bioeng. 106 (2010) 247–259. doi:10.1002/bit.22690.

[59]   F. De Jaeghere, E. Allémann, J.C. Leroux, W. Stevels, J. Feijen, E. Doelker, R. Gurny, Formulation and lyoprotection of poly(Lactic acid-co-ethylene oxide) nanoparticles: Influence on physical stability and In vitro cell uptake, Pharm. Res. 16 (1999) 859–866. doi:10.1023/A:1018826103261.

[60]   N. Shamim, L. Hong, K. Hidajat, M.S. Uddin, Thermosensitive-polymer-coated magnetic nanoparticles: Adsorption and desorption of Bovine Serum Albumin, J. Colloid Interface Sci. 304 (2006) 1–8. doi:10.1016/j.jcis.2006.08.047.

[61]   M.J. Santander-Ortega, N. Csaba, L. González, D. Bastos-González, J.L. Ortega-Vinuesa, M.J. Alonso, Protein-loaded PLGA-PEO blend nanoparticles: Encapsulation, release and degradation characteristics, Colloid Polym. Sci. 288 (2010) 141–150. doi:10.1007/s00396-009-2131-z.

[62]   T. Morita, Y. Sakamura, Y. Horikiri, T. Suzuki, H. Yoshino, Protein encapsulation into biodegradable microspheres by a novel S/O/W emulsion method using poly(ethylene glycol) as a protein micronization adjuvant, J. Control. Release. 69 (2000) 435–444. doi:10.1016/S0168-3659(00)00326-6.

[63]   L.J. White, G.T.S. Kirby, H.C. Cox, R. Qodratnama, O. Qutachi, F.R.A.J. Rose, K.M. Shakesheff,

Accelerating protein release from microparticles for regenerative medicine applications, Mater. Sci. Eng. C. 33 (2013) 2578–2583. doi:10.1016/j.msec.2013.02.020.

[64] I.J. Castellanos, W. Al-Azzam, K. Criebenow, Effect of the covalent modification with poly(ethylene glycol) on α-chymotrypsin stability upon encapsulation in poly(lactic-co-glycolic) microspheres, J. Pharm. Sci. 94 (2005) 327–340. doi:10.1002/jps.20243.

[65] K.D. Hinds, K.M. Campbell, K.M. Holland, D.H. Lewis, C.A. Piché, P.G. Schmidt, PEGylated insulin in PLGA microparticles. In vivo and in vitro analysis, J. Control. Release. 104 (2005) 447–460. doi:10.1016/j.jconrel.2005.02.020.

[66] S. Hermeling, D.J.A. Crommelin, H. Schellekens, W. Jiskoot, Structure-immunogenicity relationships of therapeutic proteins, Pharm. Res. 21 (2004) 897–903. doi:10.1023/B:PHAM.0000029275.41323.a6.

[67] C. Maas, S. Hermeling, B. Bouma, W. Jiskoot, M.F.B.G. Gebbink, A role for protein misfolding in immunogenicity of biopharmaceuticals, J. Biol. Chem. 282 (2007) 2229–2236. doi:10.1074/jbc.M605984200.

[68] J. Park, P.M. Fong, J. Lu, K.S. Russell, C.J. Booth, W.M. Saltzman, T.M. Fahmy, PEGylated PLGA nanoparticles for the improved delivery of doxorubicin, Nanomedicine Nanotechnology, Biol. Med. 5 (2009) 410–418. doi:10.1016/j.nano.2009.02.002.

[69] J. Liu, S.M. Zhang, P.P. Chen, L. Cheng, W. Zhou, W.X. Tang, Z.W. Chen, C.M. Ke, Controlled release of insulin from PLGA nanoparticles embedded within PVA hydrogels, J. Mater. Sci. Mater. Med. 18 (2007) 2205–2210. doi:10.1007/s10856-007-3010-0.

[70] M. Xia, R. Huang, K.L. Witt, N. Southall, J. Fostel, M.H. Cho, A. Jadhav, C.S. Smith, J. Inglese, C.J. Portier, R.R. Tice, C.P. Austin, Compound cytotoxicity profiling using quantitative high-throughput screening, Environ. Health Perspect. 116 (2008) 284–291. doi:10.1289/ehp.10727.

[71] C. Maupas, B. Moulari, A. Béduneau, A. Lamprecht, Y. Pellequer, Surfactant dependent toxicity of lipid nanocapsules in HaCaT cells, Int. J. Pharm. 411 (2011) 136–141. doi:10.1016/j.ijpharm.2011.03.056.

[72] G. Le Roux, H. Moche, A. Nieto, J.P. Benoit, F. Nesslany, F. Lagarce, Cytotoxicity and genotoxicity of lipid nanocapsules, Toxicol. Vitr. 41 (2017) 189–199. doi:10.1016/j.tiv.2017.03.007.

[73] M. Partearroyo, H. Ostolaza, Surfactant-induced cell toxicity and cell lysis: a study using B16 melanoma cells, Biochem. …. (1990) 1323–1328. doi:10.1016/0006-2952(90)90399-6.

FIGURE CAPTIONS

Figure 1. ^{1}H-NMR of PLGA-COOR and PEG-PLGA co-polymer in deuterated DMSO and chloroform respectively.

Figure 2. Effect of (A) NaCl and (B) lysozyme concentrations on lysozyme precipitation efficiency. For (A), lysozyme concentration was fixed at 10 mg/mL whereas NaCl concentration was fixed at 0.15 M for (B). Statistical analysis was conducted to investigate any significant difference (P ≤ 0.05) in comparison to 0.15 M NaCl or 5 mg/mL lysozyme concentration for (A) and (B) respectively. **** indicates P ≤ 0.0001, n = 3 for each lysozyme precipitation condition.

Figure 3. Scanning electronic microscopy of (A) lysozyme and (B) SDF-1α nanoprecipitates.

Figure 4. Morphology of PLGA/PEG-PLGA nanoparticles. SEM and TEM images of (A, C) unloaded and (B, D) SDF-1α-loaded nanoparticles. (E) AFM image of SDF-1α-loaded nanoparticles.

Figure 5. Release study of lysozyme. (A) Cumulative release of lysozyme in 0.05 M Tris-HCl buffer at pH 7.4 and (B) concurrent changes in the zeta-potential value of different nanoparticle formulations. Nanoparticle suspension was diluted 200-fold in 0.01 M NaCl solution and the pH was adjusted to pH 7 prior to zeta-potential measurement. (C) Cumulative lysozyme release in 0.01 M citrate buffer at pH 4.0 or (D) 0.05 M Tris-HCl buffer at pH 7.4 containing 0.15 M NaCl. Each data point with error bar represents mean ± SD, n = 3 for each formulation.

Figure 6. Release study of SDF-1α and its biological activity assessment. (A) Cumulative release of SDF-1α in 0.05 M Tris-HCl buffer at pH 7.4 containing 0.15 M NaCl. Each data point with error bar represents mean ± SD, n = 4 for each formulation. (B) Distance migrated by U87-MG cells induced by the culture medium alone (Blank), or supplemented with 40 ng/mL native, precipitated or released SDF-1α collected from Formulation 8 at different time points of the release study. Statistical analysis was conducted to investigate any significant difference (P ≤ 0.05) in comparison to the native SDF-1α. **** indicates P ≤ 0.0001, n = 3 for each type of SDF-1α treatment. (C) Examples of optical microscopic images of U87-MG cell-laden agarose drops after 72 h treatment with culture medium alone (top left) or medium containing 40 ng/mL native (top right), precipitated (bottom left) or released SDF-1α (bottom right).
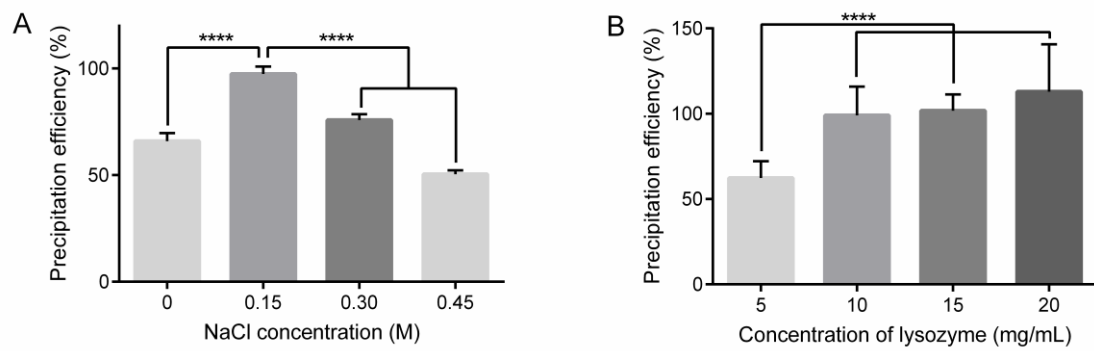
Figure 7. Effect of different concentrations of PLGA/PEG-PLGA nanoparticles (Formulation 8), lipid nanocapsules (LNC) and polystyrene (PS) nanoparticles on the viability of NIH3T3 cells after 48h incubation. n = 3 for each nanoparticle treatment.
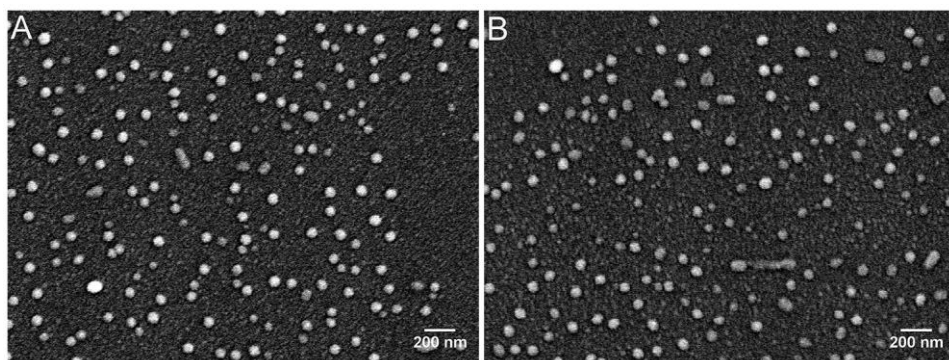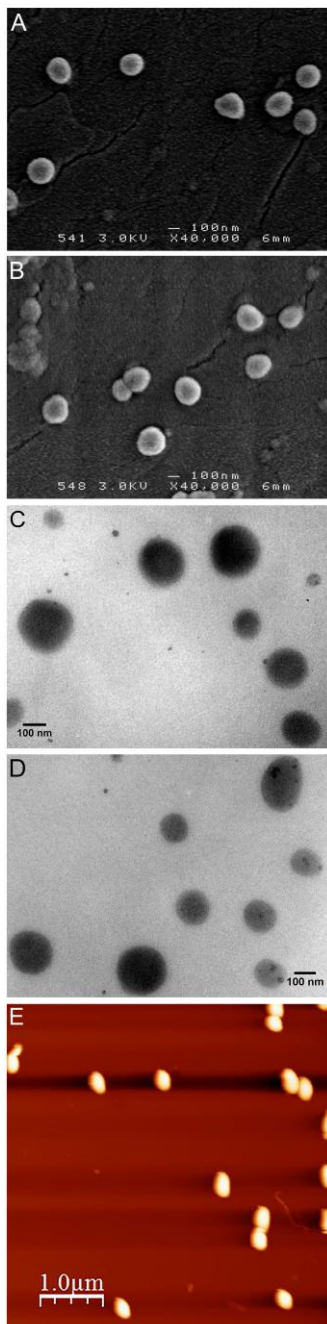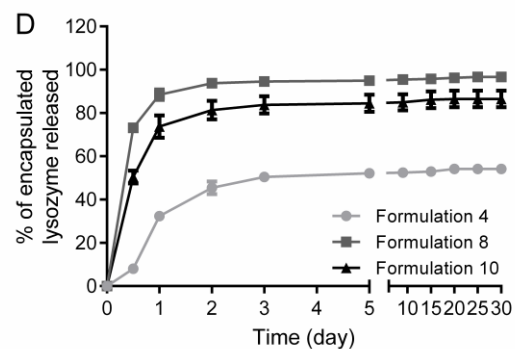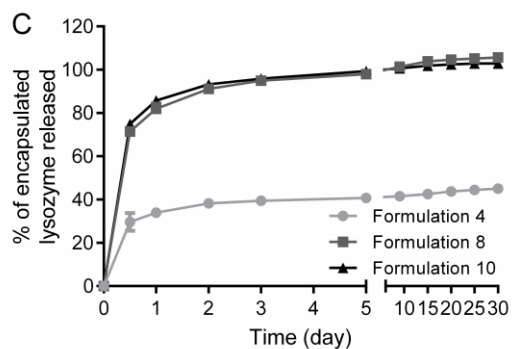
PLGA-COOR

PEG-PLGA

A

B

C
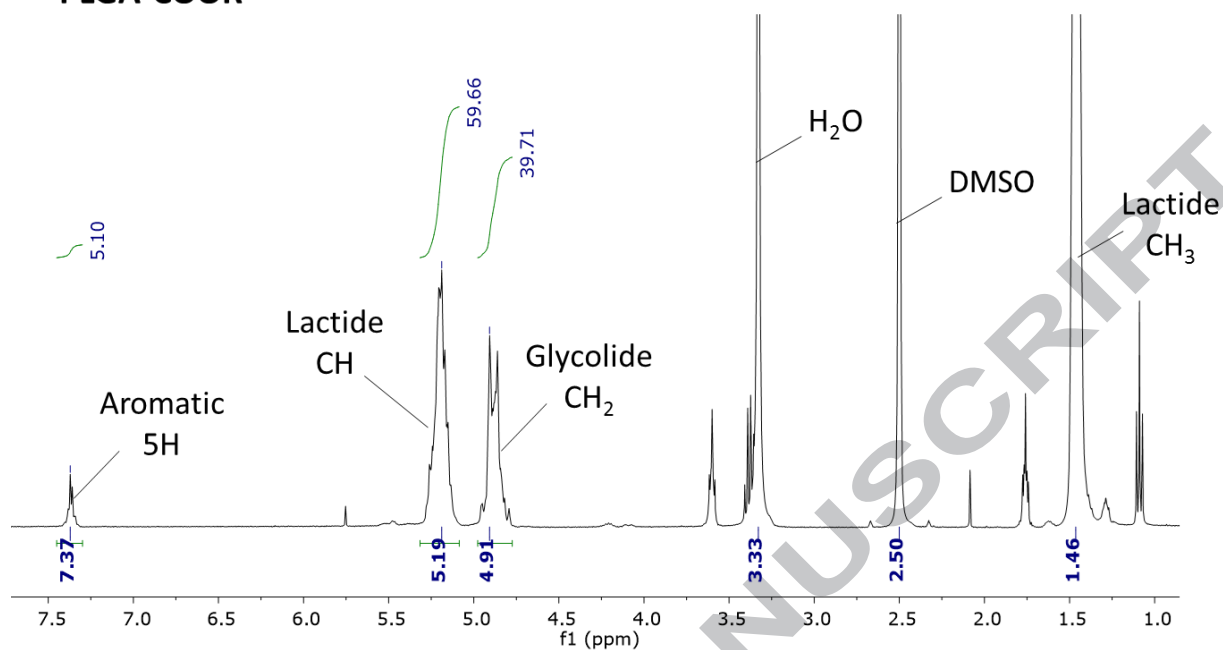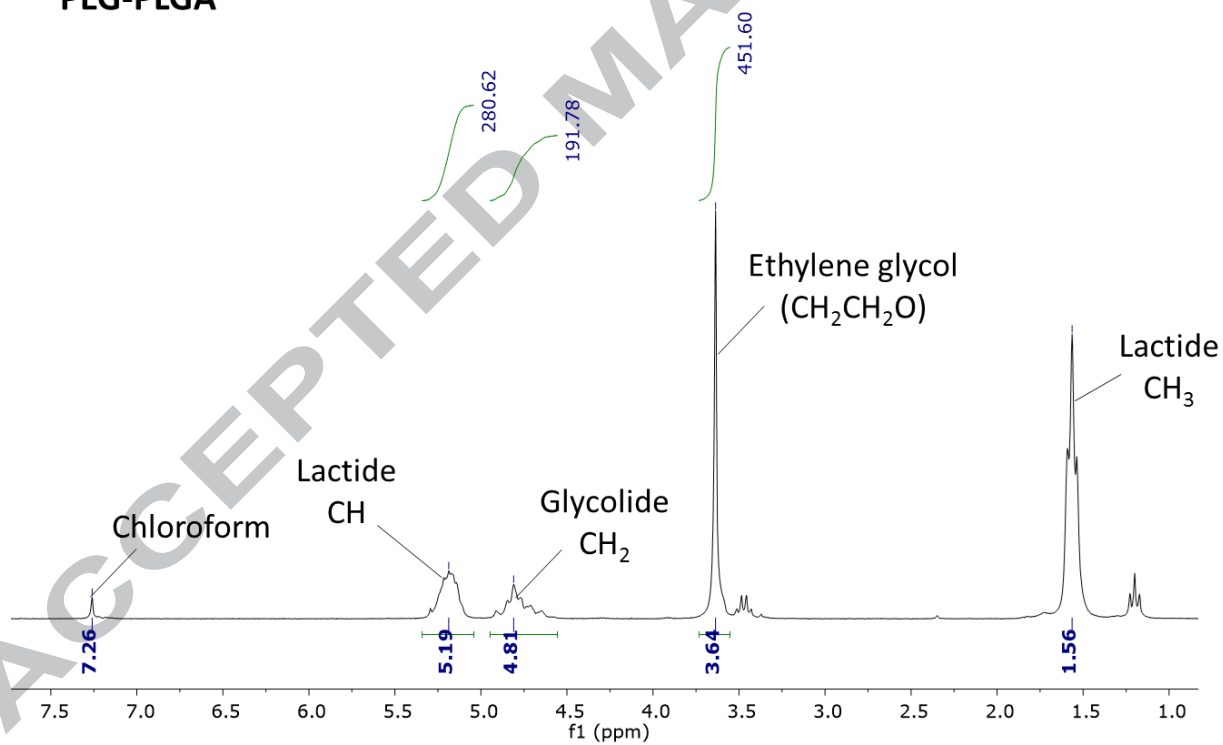
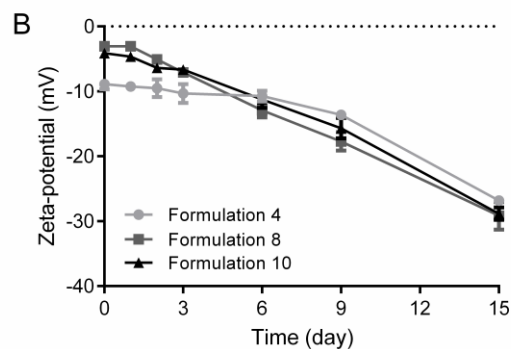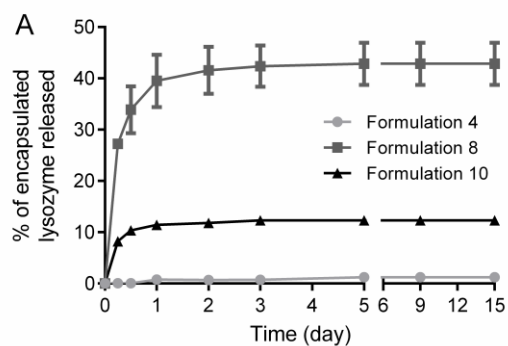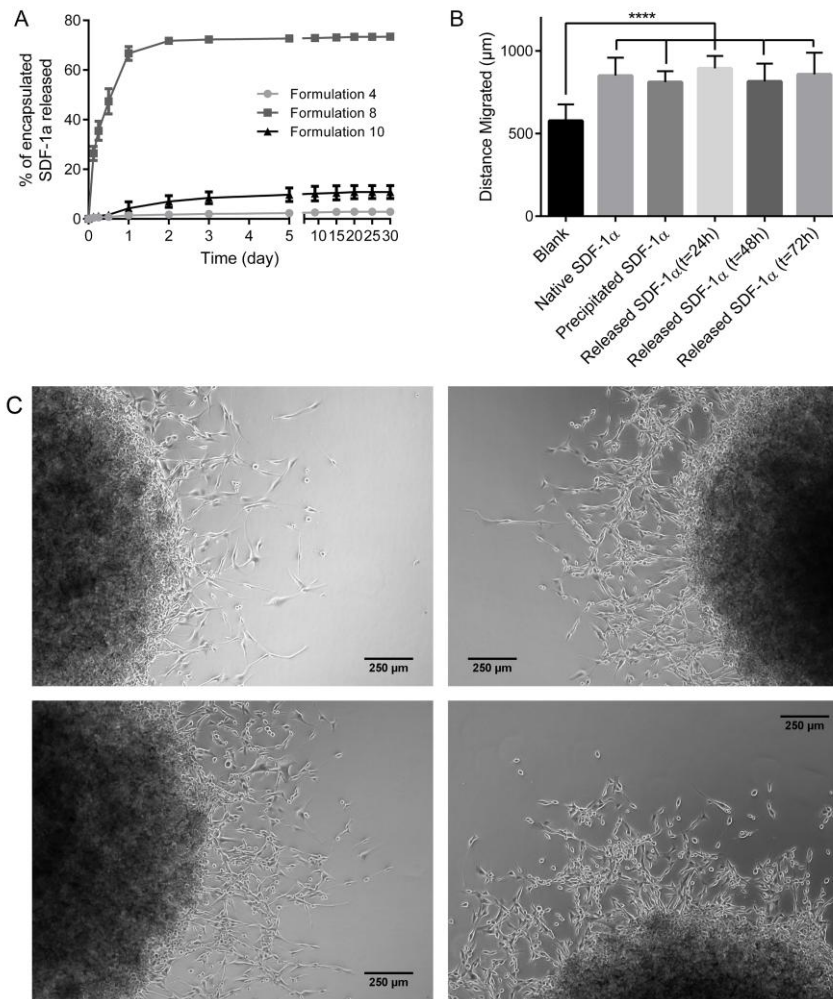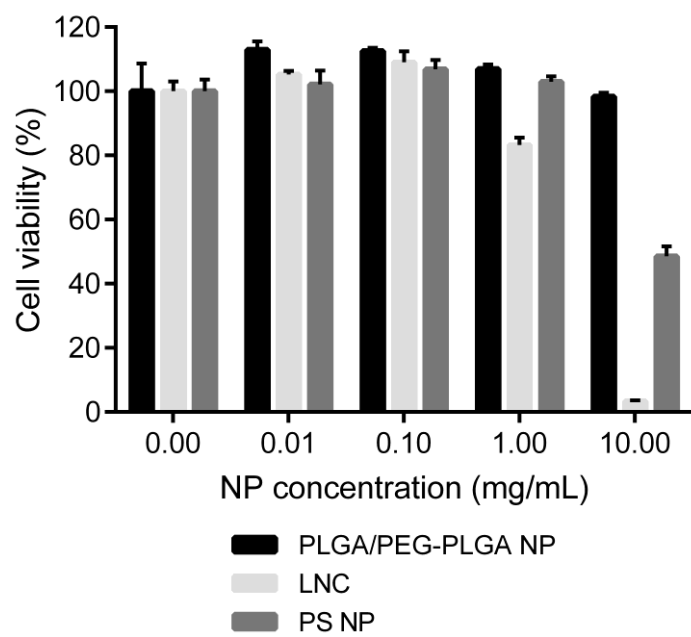**Table 1.** Average size, polydispersity index (PDI) and zeta-potential (ZP) of unloaded nanoparticle formulations. Data are presented as mean ± SD, n = 3.

Formulation number	Proportion (%)			Average size (nm)[a]	Average PDI[a]	Average ZP (mV)[b]		
	PLGA-COOH	PLGA-COOR	PEG-PLGA			pH 4	pH 7	pH 10
1	100	0	0			n.d.[c]		
2	92	0	8	599 ± 20	0.46 ± 0.08	-16.6 ± 1.0	-20.7 ± 2.2	-28.0 ± 2.4
3	75	0	25	279 ± 3	0.17 ± 0.03	-9.9 ± 0.8	-12.1 ± 1.3	-15.7 ± 1.5
4	67	0	33	202 ± 3	0.08 ± 0.05	-6.6 ± 1.0	-8.9 ± 0.8	-9.8 ± 0.7
5	0	100	0			n.d.[c]		
6	0	92	8	>1000	1	-2.9 ± 0.5	-4.7 ± 0.4	-6.4 ± 0.6
7	0	75	25	691 ± 23	0.40 ± 0.05	-1.8 ± 0.1	-2.3 ± 0.3	-3.1 ± 0.4
8	0	67	33	255 ± 4	0.14 ± 0.04	-1.2 ± 0.2	-3.0 ± 0.6	-2.9 ± 0.2
9	33	33	33	215 ± 7	0.10 ± 0.03	-4.1 ± 0.2	-4.8 ± 0.5	-4.3 ± 0.3
10	17	50	33	236 ± 6	0.10 ± 0.02	-2.8 ± 0.4	-4.1 ± 0.6	-4.0 ± 0.4

[a] Purified nanoparticle suspension was diluted to 100 µg/mL in water prior to measurement
[b] Purified nanoparticle suspension was diluted to 100 µg/mL in 0.01 M NaCl and 0.1 M HCl or NaOH was used to adjust the pH of the suspension to pH 4, 7 or 10 prior to measurement
[c] n.d. = not determined, as no homogenous particle suspension was obtained

Table 2. Characterization of PLGA/PEG-PLGA nanoparticles (Formulation 8) before and after freeze-drying without any cryoprotectant or with sucrose, trehalose or HPBCD. Data are presented as mean ± SD, n = 3.

Protectant	Average size (nm)		Average PDI		S_f/S_i	PDI_f/PDI_i
	Before freeze-drying[a]	After freeze-drying[b]	Before freeze-drying[a]	After freeze-drying[b]		
-		n.d.[c]			n.d.[c]	
Sucrose	255 ± 8	308 ± 5	0.13 ± 0.01	0.22 ± 0.01	1.21	1.69
Trehalose		266 ± 5		0.19 ± 0.01	1.04	1.46
HPBCD		255 ± 3		0.14 ± 0.02	1.00	1.08

[a] Purified nanoparticle suspension was diluted to 100 µg/mL in water prior to measurement
[b] Freeze-dried nanoparticles were re-suspended in 2 mL water and diluted to 100 µg/mL in the same diluent prior to measurement
[c] n.d. = not determined, as the freeze-dried product could not be reconstituted completely even after 10 minutes sonication

Table 3. Effect of pH of aqueous phase on encapsulation efficiencies of lysozyme. Data are presented as mean ± SD, n = 3.

Formulation number	pH of aqueous phase[a]	Encapsulation efficiency (%)	
		Lysozyme	SDF-1a
4	8.4	18.0 ± 0.8	34.3 ± 3.7
	9.4	28.1 ± 1.7	79.7 ± 4.1
	10.4	66.0 ± 1.6	107.7 ± 1.5
	11.4	107.0 ± 3.6	-

[a] 0.05 M glycine-NaOH buffer solution was used as the aqueous phase

Table 4. Effect of the PLGA-COOH proportion on encapsulation efficiencies of lysozyme and SDF-1α. Data are presented as mean ± SD, n = 3 and 4 for lysozyme and SDF-1α respectively.

Formulation number	PLGA-COOH proportion (%)	Encapsulation efficiency (%)	
		Lysozyme	SDF-1a
4	67	107.0 ± 3.6	107.7 ± 1.5
8	0	89.6 ± 5.7	75.5 ± 2.2
9	33	108.2 ± 1.9	-
10	17	111.0 ± 3.9	104.0 ± 2.8

Table 5. Average size, polydispersity index (PDI) and zeta-potential (ZP) of lysozyme and SDF-1α-loaded nanoparticles. Data are presented as mean ± SD, n = 3.

Formulation number	Encapsulated protein	Average size (nm)[a]	Average PDI[a]	Average ZP (mV)[b]
4	Lysozyme	202 ± 5	0.09 ± 0.01	-9.7 ± 0.8
	SDF-1α	197 ± 2	0.08 ± 0.01	-9.6 ± 0.7
8	Lysozyme	253 ± 5	0.17 ± 0.03	-3.3 ± 0.3
	SDF-1α	259 ± 8	0.19 ± 0.01	-2.9 ± 0.2

[a] Purified nanoparticle suspension was diluted to 100 μg/mL in water prior to measurement

[b] Purified nanoparticle suspension was diluted to 100 μg/mL in 0.01 M NaCl solution and the pH of the suspension was adjusted to pH 7 prior to measurement
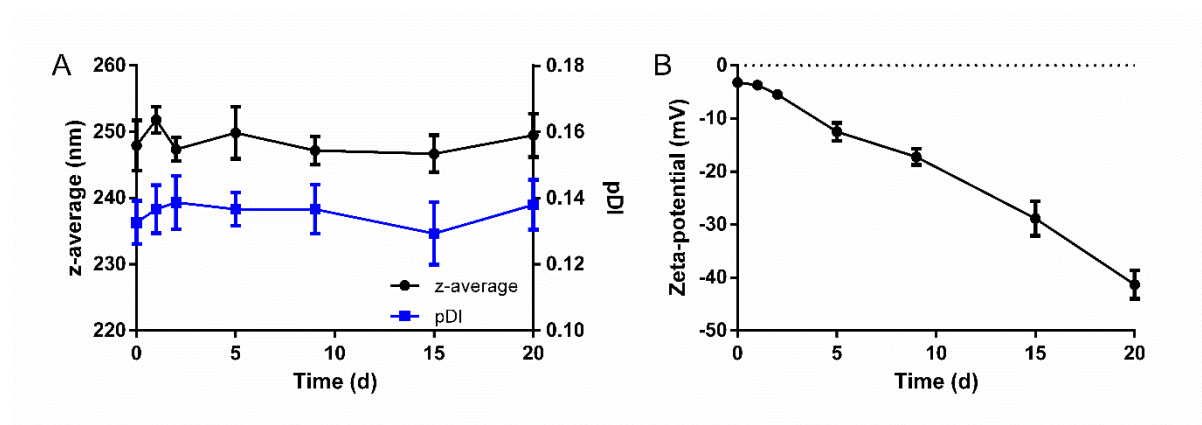
Supplementary Materials

Figure S1. Changes in average size and pDI (A), and zeta potential (B) with time of incubation of 1 mg/mL PLGA/PEG-PLGA nanoparticles (Formulation 8) in 0.05 M Tris-HCl buffer (pH 7.4) at 37 °C. Each data point with error bar represents mean ± SD, n = 3. For size and pDI measurement, nanoparticle suspension was diluted in water. For zeta-potential measurement, nanoparticle suspension was diluted in 0.01 M NaCl solution and the pH was adjusted to pH 7.